Environmental Earth Sciences (2020) 79:84
https://doi.org/10.1007/s12665-020-8821-z

ORIGINAL ARTICLE

Mine water hydrogeochemistry of abandoned coal mines in the outcropped Carboniferous formations, Ruhr Area, Germany

Tuan Quang Tran[1,2] · Andre Banning[1] · Frank Wisotzky[1] · Stefan Wohnlich[1]

Received: 15 July 2019 / Accepted: 20 January 2020 / Published online: 5 February 2020

Abstract

A hydrogeochemical study was conducted in the outcropped part of the coal-bearing Upper Carboniferous formations in the Ruhr area to investigate the characteristics of regional mine water and understand the hydrogeochemical conditions. Twenty-eight mine water samples from the adits of different abandoned coal mines were collected and analyzed for major ions, iron (Fe^{2+}, Fe_{total}) and sulfide (H_2S). The water samples had a pH of 6.39–7.65. Total dissolved solids (TDS) ranged from 157 to 1806 mg L^{-1}. Mine water samples were dominated by $HCO_3^- > Ca^{2+} > SO_4^{2-} > Mg^{2+} > Na^+ > Cl^- > K^+ > NO_3^- > (F^-, Li^+)$. Several water samples had elevated SO_4^{2-}, Fe_{total}, and H_2S concentrations up to 354 mg L^{-1}, 4.2 mg L^{-1}, and 10 µg L^{-1}, respectively. The water types (Ca–Mg–HCO_3–SO_4, Na–Ca–HCO_3–SO_4, Ca–Mg–Na–HCO_3–SO_4, and Na–Ca–Mg–HCO_3–SO_4) were the dominant hydrogeochemical facies. Gypsum and halite were always undersaturated, while calcite and dolomite were undersaturated in about 82% of water samples. The chemical weathering processes of pyrite, calcite, dolomite, gypsum, and halite, as well as ion exchange, appear to be the dominant hydrogeochemical processes controlling adit mine water chemistry. In general, there was an increasing trend of TDS and major ion concentrations from south to northeast in the study area. This study may aid in the improvement of water management in the Ruhr area since the adits discharge into the river Ruhr which is strongly used for the drinking water supply of a large metropolitan region in western Germany.

Keywords Coal-mining · Water–rock interaction · Weathering · Ion exchange

Introduction

Abandoned coal mine drainage is a common kind of polluted water in coal mine areas, caused by coal mining operations in the past. Mine water from the ceased underground mines can be released through adits, fractures, and fissures, reaching the earth's surface (Ceto and Mahmud 2000). In terms of chemistry, the abandoned mine drainage can be divided into several different categories, such as acid, alkaline, neutral and metalliferous mine drainage (Younger 1995; Johnson 2003; Pope et al. 2010; Nordstrom 2011; Favas et al. 2016). Acid mine drainage is characterized by a low pH value (Favas et al. 2016). The alkaline mine drainage typically occurs when the carbonate minerals, such as calcite or dolomite are present in the mining areas (Bigham and Nordstrom 2000; Gomo 2018).

Mine drainage is one of the important issues for both mining operation stages and closed or abandoned mines (Russo et al. 2013). It is a cause for the community concerns and environmental problems in many parts of the world (Favas et al. 2016), especially contaminated water from abandoned mines (Kgari et al. 2016). Coal mine drainage problems can continue in many years after ceasing mining operations (Powell 1988). Water exists and circulates in the mine galleries of abandoned mines and promotes the sulfide oxidative weathering and the effluents with high pollution potential can migrate to various natural systems (Favas et al. 2016). For active mines, mine water is often treated to minimize environmental impacts. On the contrary, it can discharge in an uncontrolled manner by abandoned mines, resulting in widespread mine drainage pollution problems (Younger 1995). Many coal mines have ceased mining with the problems of mine drainage. For instance, abandoned coal mine drainage may be contaminated and seriously affected on the

✉ Tuan Quang Tran
quang.tran@rub.de; tranquangtuan@humg.edu.vn

[1] Hydrogeology Department, Faculty of Geosciences, Ruhr-Universität Bochum, Universitätsstr. 150, 44801 Bochum, Germany

[2] Faculty of Geosciences and Geoengineering, Hanoi University of Mining and Geology, Hanoi, Vietnam

water quality, aquatic life, ecological and drinking water resources and they were reported by many researchers in the world (Powell 1988; Bigham and Nordstrom 2000; Younger et al. 2002; Bott et al. 2012; Opitz and Timms 2016). Degradation of groundwater and surface water quality have also occurred by acid mine drainage in abandoned coal mine areas of South Africa and the United States (Mayo et al. 2000; Kgari et al. 2016). Drainage waters from abandoned coal mines carried mechanical suspension to the surrounding landscape (Krechetov et al. 2019).

For those reasons, many studies have been conducted on the hydrogeochemical characterization of mine drainage to evaluate the mining environment impact (Favas et al. 2016), as well as quality evaluation of abandoned mine drainage through the potential sources of dissolved substances. Wolkersdorfer (2009) studied the hydrogeochemical characteristics of mine water, which drainages from the dewatering adits of abandoned underground coal mines in the Upper Bavarian coalfield district, Germany. The hydrogeochemical facies of mine water have been identified as Ca–HCO_3, with some Ca–Mg–SO_4 and mine water had a noticeable H_2S smell. At least six coal mine water discharge sites were determined, which were the cause of a local negative impact on the receiving streams. The major controlling factors for mine water chemistry of coal mines were studied, including pyrite weathering (Wolkersdorfer 2009). The high concentrations of major ions (SO_4^{2-}, Cl^-, Na^+, Mg^{2+}, K^+, and Ca^{2+}) of abandoned coal mine water from different discharge points in the Witbank coalfield, in South Africa, were demonstrated by Kgari et al. (2016). Hydrogeochemistry studies of coal mine drainage in North Derbyshire and South Yorkshire coalfields, UK showed that abandoned coal mine water was acidic or alkaline and contained high sulfate concentrations. Major ions chemistry can shed light on some factors of the geochemical processes that control the composition of mine water (Banks et al. 1997). Another research was carried out by Bozau et al. (2017) on the hydrogeochemistry of mine water of abandoned ore mines in the Harz mountains, northern Germany. The quality of mine water can be explained by leaching of ore minerals, and the origins of major ions were from halite dissolution, silicate weathering and ion exchange processes (Bozau et al. 2017).

In general, there are many studies on coal mine drainage in the whole Ruhr area. For example, Coldewey and Semrau (1994) presented the history of coal mine drainage. Müller (2016) reported that in the central and northern parts of the Ruhr coal area, groundwater is used for the production of drinking water. Thus, mine water still needs to be pumped to the surface to prevent groundwater contamination by the intrusion of water with high salinity and mineralization in the depths of the mines (Müller 2016). The pumping rate for coal mine drainage was 66.3 million m^3 in 2016 for the whole Ruhr coalfield (Drobniewski et al. 2017). These studies have provided an overview of coal mine drainage in the whole Ruhr area. However, in the study area here, there is very little published research on coal mine water, especially on the hydrogeochemistry of abandoned coal mine drainage. Previously published data (Wisotzky 2017) referred to the water chemistry of several water adits in the southern Ruhr area. Abandoned coal mine drainage is not treated and drained directly to the Ruhr river and its tributaries through the adits of the mines (Wisotzky 2017). So far, there has been no detailed and systematic study of the hydrogeochemical parameters of abandoned coal mine drainage in the study area. Therefore, this study was developed with three main goals, (1) to create an inventory of the discharge sites of abandoned coal mines, and to collect mine water samples; (2) to describe the chemical composition of mine waters; (3) to identify the hydrogeochemical processes controlling the dissolved constituents of mine water.

Understanding of the hydrogeochemical conditions of abandoned coal mine drainage is a basis for providing important information, such as the status of mine water quality, serving the regional development planning and drinking water management. Furthermore, results are used for evaluating the impact of mine water in the hydrochemical cycle of the Ruhr area, Germany.

Study area

Hard coal mining in the Ruhr area, Germany, started in medieval times and decommissioned at the end of 2018 (Goerke-Mallet et al. 2016a; Drobniewski et al. 2017). A new stage of this industry, the post-mining and the rehabilitation of the mining environment, are taking place continuously. The Ruhr coal mining area is located in the Ruhr valley and divided into (1) sub-surface, (2) near-surface and (3) deep-level mining areas (Goerke-Mallet et al. 2016b). The study area is the outcropped part of the coal-bearing Upper Carboniferous formations on the surface and is situated on (1), and a small part on (2), representing areas of early shallow mining in the south, a part of the eastern and western areas of the Ruhr river valley. It covers an area of approximately 754 km^2, with 50 km in east–west length and 15 km north–south width (Drozdzewski et al. 2008; Fig. 1), spreading over Hattingen, Sprockhövel, Witten, Wetter and Schwerte cities, and parts of Essen, Bochum, Dortmund, Holzwickede and Herdecke cities, with a total of approximately 1.8 million people (Statistics and IT services NRW 2018). It has a long history of coal extraction dating back to the thirteenth century (Harnischmacher 2010; Henkel and Melchers 2017), and all mining activities in the study area stopped in the 1960s (Drobniewski et al. 2017). Although coal mines and

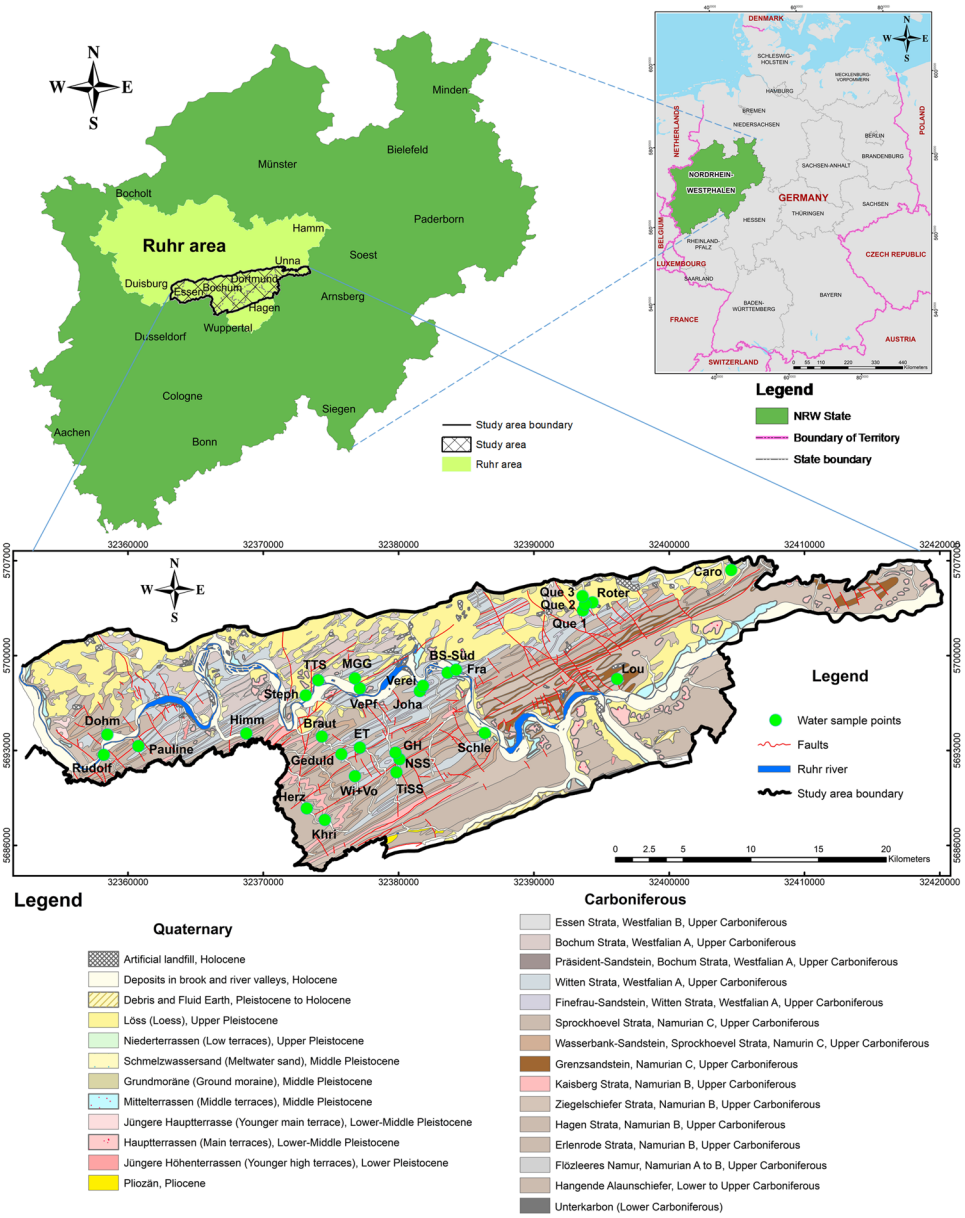

Fig. 1 Location and geological maps of the study area and sampling sites (modified from the GD.NRW-WMS 2017)

collieries are abandoned, their water discharge adits are still accessible. They are called with the names "Stollen" or "Erbstollen" by the German language.

The topography is generally shallow hills and the elevation gently ranges between about 20 and 330 m above sea level (a.s.l.). The lowest elevation points are along the downstream of the Ruhr river, in Mülheim city (about 20–30 m a.s.l.). The highest elevation points are located in Hattingen (e.g. Oberelfringhausen), in Sprockhövel (e.g. Holthausen), with the elevation of about 330 m a.s.l. The Ruhr river runs from east to west and is the main tributary of the area. The study area is characterized by mild winters and cool summers. According to observational data (Bochum, Essen-Bredeney and Gevelsberg-Oberbröking climate stations, in the study area, 2008–2018), the annual average temperature was 10.4 °C. The annual mean precipitation in the region was 891 mm in the same observation period (DWD 2019).

In the whole Ruhr area, the Upper Carboniferous strata (Namurian to Westphalian) crop out directly on the surface (Fig. 1) or are underneath thin overlying sediments of Quaternary age and overlain by thick sediments of Cretaceous age in the north (Strehlau 1990; Littke et al. 1994; Drobniewski and Witthaus 2017; Frankenhoff et al. 2017; Zieger et al. 2018). The Carboniferous strata have a thickness of about 3000 m and contain more than 100 coal seams with variable thicknesses (Coldewey and Semrau 1994). In the outcropped Upper Carboniferous formations, coal seams started in the Namurian C and reached maximal capacity in the Westphalian A and B (Littke and Ten Haven 1989; Drozdzewski 1993). Genetically, the strata

represent cyclothems and consist alternate layers of thick sandstone, silt-, mud-, and claystone layers, which contain clay minerals (kaolinite, chlorite, biotite), feldspar (albite, anorthite), siderite, dolomite, calcite, quartz, and pyrite (Strehlau 1990; Wisotzky 2017) with interspersed coal seams. Particularly, these formations include strata with the following local names from stratigraphic top to bottom as follows: In Namurian B deposits, the main outcropped strata (Kaisberg, Ziegelschiefer, Hagen, and Erlenrode), cover the western, southern and eastern parts of the study area. The strata are generally composed of clay, claystone, siltstone, mudstone, subordinate sandstone, sandstone layers (quartz, rich in mica minerals), and locally conglomerate. The first thin coal seams developed in coastal swamps (in Kaisberg formation) (GD.NRW-WMS 2017). The Namurian C deposits (Sprockhövel strata) cropped out mostly in the central part of the study area. It is composed of dark gray sandstone (feldspar, quartz, calcite, pyrite), siltstone and mudstone layers. The thicknesses of the coal seams reach from 0.5 to 1 m. In the Westphalian A deposits (Bochum and Witten strata) which are situated in the south of Essen, Bochum, in the Sprockhövel and Holzwickede areas and the central part of Dortmund. They are composed of sandstone, siltstone (silica, calcite and iron oxides) and mudstone layers, with numerous hard coal seams with thicknesses of 1–2 m. Feldspars, calcite, mica, quartz, and iron oxide minerals are common minerals in the rocks. The Westphalian B deposits (Essen strata) are widely distributed in the study area but only outcrop as a small part in Wiemelhausen, Bochum. The strata are characterized by siltstone and mudstone layers, with numerous hard coal seams which have thicknesses of 1–2 m (Drozdzewski et al. 2008). The Upper Carboniferous hard coal deposits were affected by tectonic movement at the end of the Variscan orogenesis and intensely folded in the Late Carboniferous (Gielisch 2010). Deposits of Pliocene and Pleistocene ages are present in only a small part, overlying the Upper Carboniferous formations, including boulder clay to loess and loess clay to coarse-sandy terrace gravel (Coldewey and Semrau 1994). Holocene deposits consist of sediments from Ruhr river and its tributaries, including clay, fine sand and silt with deposits of melt-water and loess, and artificial landfill materials (GD.NRW-WMS 2017).

Sample collection and methods

Twenty-eight mine water samples for hydrogeochemical analysis were collected from the different drainage sites from the portal of the adits of abandoned coal mines in the study area from January to March 2018 (Fig. 1). At each of the sampling sites, pH, oxidation–reduction potential (ORP) and electrical conductivity (EC) values were determined using the WTW and Consort portable meters. The EC and pH values were measured using a WTW Multi350i meter, while ORP value was measured by a WTW-pH340 meter (WTW, Weilheim, Germany). The probes were calibrated in the laboratory using standard solutions on the sampling day. Samples were collected in 250 mL glass bottles for HCO_3^- and H_2S analyses and in 25 mL PE bottles for Fe^{2+} and Fe_{total} analyses. Samples for major ions analysis were filtered in the field through 0.45 µm Millipore cellulose acetate membrane filters into 50 mL PE bottles, filled to the top and tightly capped. Samples for cation analysis were preserved and acidified to pH < 2 with ultra-purified HNO_3 (1%).

Water samples were analyzed in the Hydrochemistry laboratory, Institute of Geology, Mineralogy and Geophysics, Ruhr University Bochum. The acid titration method (HCl) was used to determine the concentration of HCO_3^-. To assure the quality of results, titrations were conducted twice to triplicate in the laboratory on the day after field sampling. Fe^{2+}, Fe_{total}, and H_2S concentrations were measured using 551S UV/VIS Spectrophotometer (LAMPS) (Perkin-Elmer GmbH, Berlin, Germany). Major anions (SO_4^{2-}, Cl^-, NO_3^-, and F^-) were analyzed using the Ion Chromatography System, model ICS-1000 (DIONEX-Thermo Fisher Scientific GmbH, Dreieich, Germany). Major cations (Ca^{2+}, Mg^{2+}, Na^+, K^+, and Li^+) were analyzed by CD25 Conductivity Detector System (DIONEX-Thermo Fisher Scientific GmbH, Dreieich, Germany). The analytical precision was maintained by running a known standard after every four samples. Samples were stored in the refrigerator at 4 °C until completed analyses. The analyzed ions precision for all samples was determined by calculating the ionic balance error, within 5%.

The Piper diagram was used for identifying the main hydrogeochemical facies and evaluating the percentage composition of major ions. With respect to understanding the mechanisms controlling the composition of mine drainage, Gibbs diagrams were used. The weight ratios of $Na^+/(Na^+ + Ca^{2+})$ and $Cl^-/(Cl^- + HCO_3^-)$ as a function of TDS (mg L^{-1}) were plotted to represent the Gibbs cation and Gibbs anion diagrams. Various researchers have already demonstrated the usefulness of Gibbs diagrams for groundwater in general (Lakshmanan and Kannan 2003; Glover et al. 2012; Li et al. 2013; Huang et al. 2018), and for mine water in particular (Tiwari et al. 2016c). Therefore, this study also used the Gibbs diagrams to investigate the processes governing mine water chemistry. The Piper and Gibbs diagrams were presented using Geochemist's Workbench 12.0 software. Series scatter charts were plotted using OriginPro 8.5.1 software and Microsoft Excel. The major ion concentrations were plotted on the Stiff diagrams using AquaChem 2014.2 software and depicted in the map for spatial distributions by comparing their dominant ions. The PHREEQC 3.4 geochemical software was used to describe the main hydrogeochemical processes and calculate the

saturation indices of calcite (SI_{cal}), dolomite (SI_{dol}), gypsum (SI_{gyp}), halite (SI_{halite}), and CO_2 partial pressure log(pCO_2) value. Maps were digitized and processed using ArcGIS 10.5.1 software. The Spearman correlation coefficient was calculated using SPSS 23 software, showing the correlation between several hydrogeochemical parameters for analyzing samples.

Results and discussion

Hydrogeochemical characteristics

In the study area, there are about twenty-eight different drainage sites of the abandoned coal mines, where mine water discharges, while others are dried or buried. Hydrogeochemical results of mine water samples were summarized in Table 1, including statistical analyses, such as maximum, minimum, average values of the major ions data, Fe^{2+}, Fe_{total}, and H_2S, as well as calculated mineral saturation indices and CO_2 partial pressure.

pH, EC, ORP and TDS values

The pH values of water samples ranged from 6.39 to 7.65 with a mean value of 6.96, indicating circum-neutral conditions. The maximum pH value (7.65) was observed at Himm point in the western part and minimum pH value (6.39) was observed at TiSS site in the central part of the study area. This can be explained by the dissolution of carbonate-rich materials (Alhamed 2013) or may be influenced by the reaction with bicarbonate (Wisotzky 2017). The EC values of mine water fluctuated from 202 to 1713 µS cm^{-1} with an average value (avg.) of 790 µS cm^{-1}. Compared with the EC values of the Ruhr river water (from 100 to 570 µS cm^{-1}) that studied by Stögbauer et al. (2008), these values of coal mine drainage were higher than the values of the Ruhr river water. The measured EC value of mine water at the Roter adit, in Dortmund (located in the northeastern part), reached the highest value (1713 µS cm^{-1}), while the minimum EC value was observed in sample Wi + Vo (202 µS cm^{-1}), in Sprockhövel (in the southern part of this area). The ORP values ranged from − 12 to 444 mV (Eh values from 193 to 649 mV), indicating predominantly oxidizing conditions. The different TDS values may be reflected by the variation in geochemical processes, prevailing hydrological regime, and lithology (Singh et al. 2010; Wohnlich 2012; Tiwari et al. 2016b). TDS values in the mine water ranged between 157 and 1806 mg L^{-1} (avg. 798 mg L^{-1}). Based on Table 1, the TDS value was the highest at the Roter site (reached maximum value of 1806 mg L^{-1}), followed by Que 2, Que 1 and Que 3 sites, with TDS values of 1787, 1640 and 1574 mg L^{-1}, respectively, which are located in the northeastern part of the area (Fig. 1), with a high concentration of major ions. Otherwise, at Wi + Vo site in the southern part (Fig. 1) (the highest elevation adit) was measured the minimum value (157 mg L^{-1}). In general, the TDS values increased from southern to northeastern parts of the area. The TDS values also correlated with the EC, with a correlation coefficient value = 0.93, $p < 0.01$.

Major ion chemistry

Dominant dissolved ions in mine water samples were HCO_3^-, SO_4^{2-}, Cl^-, Ca^{2+}, Mg^{2+}, and Na^+, with minor contributions from NO_3^-, F^-, K^+, and Li^+. Results showed the dominance of weak acids (HCO_3^-) and alkaline earths ($Ca^{2+} + Mg^{2+}$) of the coal mine drainage (Fig. 3; Table 1). HCO_3^-, SO_4^{2-} and Cl^- constituted 33.59, 15.96 and 5.35% of the TDS values, respectively, and Ca^{2+}, Mg^{2+} and Na^+ accounted for 9.39, 3.71 and 5.70%, respectively. K^+, Li^+, NO_3^-, and F^- contributed very little (from 0.03 to 1.67%).

The order of abundance of anions in abandoned coal mine drainage was $HCO_3^- > SO_4^{2-} > Cl^- > NO_3^- > F^-$ (Table 1). In contrast, this order for surface water outside the mining areas (Ruhr river and its tributaries) was $HCO_3^- > Cl^- > SO_4^{2-} > NO_3^-$ with the average values of 119, 56.5, 45.2, and 12.9 mg L^{-1}, respectively (Stögbauer et al. 2008). In general, concentrations of HCO_3^- and SO_4^{2-} in mine drainage were higher than of Ruhr river and its tributaries.

In the mine water samples, the concentration of HCO_3^- ranged from 36.6 mg L^{-1} (at Wi + Vo site in the southern part) to 606.9 mg L^{-1} (e.g. Roter site), constituting around 53% of the total anion concentration (TAC). HCO_3^- was the most dominant anion at the Que 1, Que 2, Que 3, Roter, and Caro sites which located in the northeastern part and at Fra site in the central part of the study area (Table 1).

The SO_4^{2-} concentrations of mine water samples extended from 24 to 354 mg L^{-1}. In equivalent units, SO_4^{2-} accounted for 31.1% of the TAC, and had the highest values at some sampling points (e.g. Que 1, Que 2, Que 3, and Roter sites in the northeastern part, with 331, 333, 354, and 336 mg L^{-1}, respectively, followed by Fra, and Joha sites in the central part of the area, with 207, and 166 mg L^{-1}, respectively).

The Cl^- concentrations in the mine water samples stretched from 10.9 to 118 mg L^{-1} and contributed 13.6% of the TAC, with an average value of 36 mg L^{-1}. The presence of Cl^- ion in mine drainage at Steph, Que 1, and Que 3 sites, which coal mines in the northern and northeastern parts, with values of 118, 62.8, 60.4 mg L^{-1}, respectively, had higher values than other sites in the southern and western parts (Khri, Herz, Wi + Wo, and Rudolf, Himm).

Table 1 Hydrogeochemical data of the analyzed coal mine water samples in the study area

Sample ID	pH	Eh	EC	TDS	HCO_3^-	SO_4^{2-}	Cl^-	NO_3^-	F^-	Ca^{2+}	Mg^{2+}	Na^+	K^+	Li^+	H_2S	Fe^{2+}	Fe_{total}	SI_{cal}	SI_{dol}	SI_{gyp}	SI_{halite}	log (pCO_2), atm
Que 1	7.15	208	1620	1640	533.8	331	60.4	< 0.1	0.2	101	43	218	11.2	< 0.5	–	–	–	0.18	0.19	− 1.13	− 6.48	− 1.44
Que 2	7.09	193	1661	1787	582.6	333	59.4	1.1	0.2	102	44	207	10.7	< 0.5	–	–	–	0.14	0.09	− 1.13	− 6.51	− 1.35
Que 3	7.30	417	1622	1574	509.4	354	62.8	1.3	0.2	93.7	45	216	11.6	< 0.5	–	–	–	0.34	0.64	− 1.15	− 6.48	− 1.58
Roter	6.97	208	1713	1806	606.9	336	59.8	< 0.1	0.2	91.4	39	251	9.9	< 0.5	–	–	–	0.01	− 0.13	− 1.18	− 6.43	− 1.2
Caro	7.28	444	934	1208	436.2	80.9	38	23	0.1	161	13	20	7.1	< 0.1	–	–	–	0.47	0.01	− 1.43	− 7.7	− 1.66
MGG	6.60	276	672	688	228.8	98.8	30	3.7	0.2	71	28	15	5.2	< 0.5	–	0.7	0.95	− 0.81	− 1.89	− 1.61	− 7.91	− 1.25
VePf	7.09	376	566	471	216.6	70.4	32	0.8	0.1	67.9	19	17.9	4.1	< 0.1	–	0.4	–	− 0.35	− 1.12	− 1.74	− 7.8	− 1.76
TTS	6.78	224	631	567	277.6	54.3	38	< 0.1	0.1	62.3	26	22.5	9.4	< 0.1	2	2	–	− 0.59	− 1.43	− 1.9	− 7.63	− 1.35
Schle	6.89	389	606	645	228.8	68.9	22	5.7	0.2	47	24	33	7.9	< 0.5	1.57	0.2	0.1	− 0.68	− 1.51	− 1.9	− 7.69	− 1.54
Pauline	6.56	251	753	835	280.6	132	28	3.8	0.1	79.8	37	22	9.0	< 0.5	3.9	1.3	1.7	− 0.74	− 1.67	− 1.47	− 7.78	− 1.13
Rudolf	6.72	329	499	587	216.6	61.3	15	2.8	0.1	55	21	10	6.5	< 0.5	6.3	0.2	0.1	− 0.8	− 1.89	− 1.87	− 8.37	− 1.39
Dohm	6.64	388	500	556	179.9	65.8	18	11.5	0.1	66.4	15	12	3.9	< 0.5	7.0	< 0.1	0.1	− 0.87	− 2.25	− 1.76	− 8.22	− 1.39
Himm	7.65	374	308	244	57.95	42	17	16.2	0.2	26	8.6	13	3.0	< 0.5	5.5	0.2	0.1	− 0.73	− 1.84	− 2.24	− 8.19	− 2.89
Braut	6.91	416	677	729	268.4	91.9	25	1.9	0.2	59.1	30	33.5	9.7	< 0.1	< 1	0.3	0.4	− 0.52	− 1.21	− 1.71	− 7.64	− 1.5
ET	6.80	249	722	775	268.4	123	16	0.7	0.2	52.4	27	57.3	9.8	< 0.1	< 1	0.6	0.7	− 0.66	− 1.43	− 1.65	− 7.6	− 1.37
Geduld	7.23	228	861	986	387.4	108	15	< 0.1	0.3	50	26	92.9	11.6	< 0.1	< 1	3.5	4.2	− 0.11	− 0.35	− 1.75	− 7.43	− 1.65
Steph	6.98	649	901	663	192.2	122	118	7.6	0.1	96.5	30	36.2	10.1	< 0.1	2.01	0.2	–	− 0.39	− 1.14	− 1.44	− 6.94	− 1.71
Lou	7.31	340	686	475	131.2	79.7	87	34	0.2	59.6	15	45	7.6	< 0.5	7.4	< 0.1	–	− 0.38	− 1.18	− 1.75	− 6.97	− 2.19
Herz	7.13	388	338	353	118.9	38	17	6.1	0.2	31.9	14	9.5	4.8	< 0.1	< 1	0.25	0.3	− 0.86	− 1.97	− 2.23	− 8.33	− 2.06
TiSS	6.39	358	448	407	103.7	48	51.3	7.0	0.2	35	15	26	3.5	< 0.5	2	< 0.1	0.1	− 1.61	− 3.44	− 2.12	− 7.42	− 1.37
Khri	7.42	393	212	196	57.95	24	10.9	13.8	< 0.1	18.6	7.9	6.8	2.7	< 0.1	< 1	0.1	0.1	− 1.1	− 2.48	− 2.59	− 8.65	− 2.66
NSS	6.57	314	570	582	176.9	97.8	30	4.6	< 0.1	50	28	14	3.7	< 0.5	1.96	0.3	0.28	− 1.1	− 2.32	− 1.73	− 7.93	− 1.33
GH	6.64	445	721	635	134.2	219	15	4.4	0.2	75.6	34	11	6.9	< 0.5	–	0.1	0.1	− 1.03	− 2.28	− 1.27	− 8.35	− 1.53
Wi + Vo	7.49	401	202	157	36.6	25	14	18.7	< 0.1	16	6.5	8.7	2.7	< 0.1	< 1	0.1	0.2	− 1.36	− 3.1	− 2.61	− 8.43	− 2.95
Verei	6.90	359	757	715	314.2	164	17	2.6	0.1	72.6	43	26	7.4	< 0.5	8.2	< 0.1	–	− 0.41	− 0.91	− 1.43	− 7.93	− 1.42
Joha	6.89	238	747	642	253.2	166	21	0.5	0.2	80.4	38	15	8.0	< 0.5	7.4	2.2	–	− 0.46	− 1.1	− 1.38	− 8.07	− 1.5
Fra	6.98	219	1433	1595	579.5	207	62.2	< 0.1	0.2	83.1	35	180	12.4	< 0.5	10	2.5	2.8	0	− 0.17	− 1.37	− 6.55	− 1.22
BS-Süd	6.60	456	772	824	268.4	141	23	3.7	< 0.1	77.9	34	23	10.5	< 0.5	0.36	< 0.1	0.1	− 0.72	− 1.64	− 1.45	− 7.84	− 1.18
Average	6.96	340	790	798	273	132	36	–	–	67	27	59	8	–	–	–	0.7	− 0.54	− 1.34	− 1.68	− 7.62	− 1.63
Max	7.65	649	1713	1806	606.9	354	118	34	0.3	161	45	251	12.4	–	10	3.5	4.2	0.47	0.64	− 1.13	− 6.43	− 1.13
Min	6.39	193	202	157	36.6	24	10.9	< 0.1	< 0.1	16	6.5	6.8	2.7	–	< 1	< 0.1	0.1	− 1.61	− 3.44	− 2.61	− 8.65	− 2.95

Units of all parameters are milligrams per liter (mg L^{-1}), except for Eh, (mV); EC, (μS cm^{-1}); SI_{cal}, SI_{dol}, SI_{gyp} SI_{halite}: the saturation indexes of calcite, dolomite, gypsum, and halite, respectively; pCO_2: CO_2 partial pressure, (atm); H_2S, (μg L^{-1})

(–): no measured

Sampling points: Que 1, adit "Eisenocker führende Quellen-Quelle Schacht 1"; Que 2, adit "Eisenocker führende Quellen-Quelle Schacht 2"; Que 3, adit "Eisenocker führende Quellen-Quelle Schacht 3"; Roter, adit "Roter Bach-RoBa"; Caro, adit "Caroliner Erbstollen"; MGG, adit "Rösche von Mit Gott gewagt"; VePf, adit "Stollen Vereinigte Pfingstblume Stollen"; TTS, adit "Treue Tiefer Stollen"; Schle, adit "Schlebuscher Erbstollen"; Pauline, adit "Pauline Stollen"; Rudolf, adit "Rudolf Stollen"; Dohm, adit "Zeche Dohm's Erbstollen"; Himm, adit "Himmelscroner Erbstollen"; Braut, adit "Stollen von Braut"; ET, adit "Edelltraut Erbstollen"; Geduld, adit "Stollen von Geduld"; Steph, adit "Stephansburger Erbstollen"; Lou, adit "Stollen Vereinigte Louise"; Herz, adit "Herzkämper Erbstollen"; TiSS, adit "Tiefer Stock und Scherenberger Stollen"; Khri, adit "Khristsieper Erbstollen"; NSS, adit "Neuer Scheller Stollen"; GH, adit "Stollen von Glückauf-Hegermann"; Wi + Vo, adit "Stollenrösche von ver. Wildenberg-Vogelbruch"; Verei, adit "Vereinigungsstollen"; Joha, adit "Johannes Erbstollen"; Fra, adit "Franziska Erbstollen"; BS-Süd, adit "Braunschweig Südflügel"

The NO_3^- concentrations were analyzed with low values (< 0.1 to 34 mg L^{-1}), except for the Lou, and Caro sites in the northern part of the study area, and Wi + Vo site in the southern part, with 34, 23, and 18.7 mg L^{-1}, respectively. F^- concentrations ranged from < 0.1 to 0.3 mg L^{-1}.

For major cations, Ca^{2+} and Mg^{2+} were the dominant ions in the cation chemistry, with an average cation concentration trend of $Ca^{2+} > Mg^{2+} > Na^+ > K^+ > Li^+$ for mine water samples (Table 1). Alkaline earths ($Ca^{2+} + Mg^{2+}$) contributed 73.8% of the total cation concentration (TCC) and dominate over the alkalis ($Na^+ + K^+$) (about 26.2% of the TCC). Concentrations of Ca^{2+} and Mg^{2+} ions fluctuated from 16 to 161 mg L^{-1}, and 6.5 to 45 mg L^{-1}, accounting for 44.7 and 29.1% of the TCC, respectively. For Ruhr river and its tributaries water outside the mining areas, this order was $Ca^{2+} > Na^+ > Mg^{2+} > K^+$, with the average values of 48.5, 43.4, 7.6, and 5.9 mg L^{-1}, respectively (Stögbauer et al. 2008). In general, concentrations of Ca^{2+}, Mg^{2+}, Na^+ and K^+ in mine drainage were higher than of Ruhr river and its tributaries.

In the mine water samples, Ca^{2+} concentrations showed remarkable values at the sampling points in the northeastern part (e.g. 161, 102, and 101 mg L^{-1} at Caro, Que 2, Que 1, respectively). The concentration of Mg^{2+} also was elevated at Que 1, Que 2, and Que 3 sites in the northeastern part, followed by Verei and Joha sites in the central part of the area. Inversely, Ca^{2+} and Mg^{2+} concentrations of water samples in the southern part (e.g. TiSS, Wi + Vo, and Khri sites) had smaller values (Table 1). Concentrations of Na^+ and K^+ ranged from 6.8 to 251 mg L^{-1}, and from 2.7 to 12.4 mg L^{-1}, respectively. Na^+ contributed 23.6%, and K^+ about 2.6% of the TCC.

Furthermore, to understand the potential trends of measured geochemical parameters, the spatial distribution of major ions in the mine water composition was shown in Fig. 2. Results showed that adits located in the northern and northeastern sections had higher concentrations of HCO_3^-, SO_4^{2-}, Na^+, Ca^{2+} and Mg^{2+} than adits in the southern part. The mine water samples collected from the adits (Que 1, Que 2, Que 3, and Caro) had a quite similar distribution of water chemistry with elevated Na^+, HCO_3^-, and SO_4^{2-} concentrations. Concentrations of the major ions of sampling points located in the central part had lower values than points in the northeastern part and these values were the lowest for the sampling sites in the southern part of the study area.

Thus, there was an increasing trend of major ions concentration from southern to northeastern part in general (Fig. 2; Table 1). This implies that water–rock interaction strongly occurred in the northeastern part of the area.

Fe^{2+}, Fe_{total}, and H_2S

Concentrations of Fe^{2+} and Fe_{total} ranged from < 0.1 (e.g. at Dohm, TiSS, Verei, and BS-Süd sites) to 3.5 mg L^{-1} (Geduld site), and from 0.1 and 4.2 mg L^{-1}, respectively. Fe^{2+} concentration had its highest value of the Geduld site in Hattingen, where maybe the oxidative weathering of sulfide-bearing minerals, such as pyrite (FeS_2) occurred. The H_2S concentration ranged between < 1 and 10 µg L^{-1} and reached the highest value at Fra site (10 µg L^{-1}). There was a positive correlation of H_2S with Fe^{2+} values

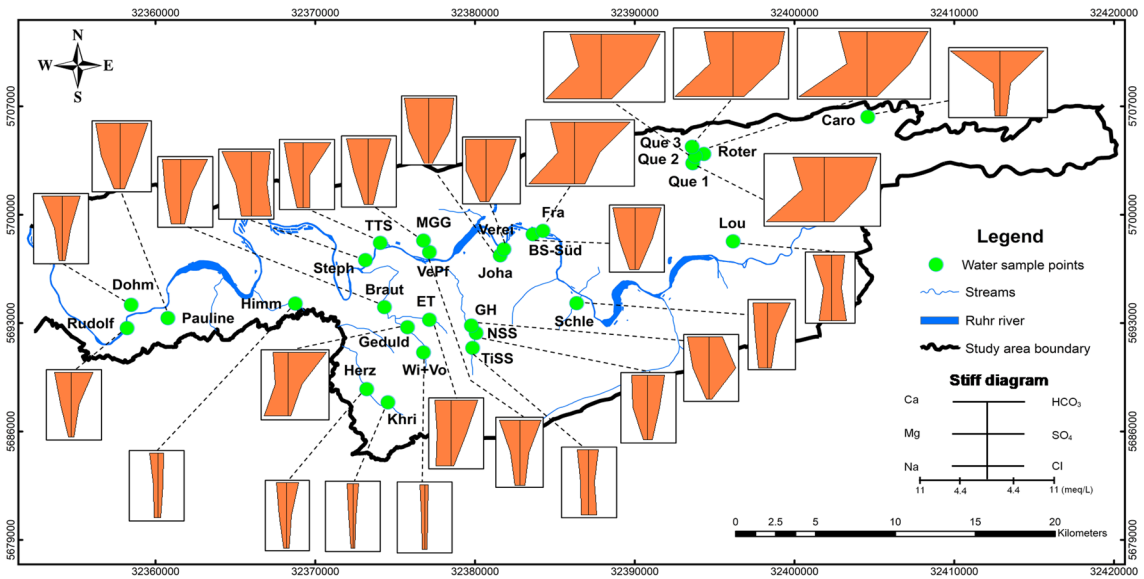

Fig. 2 Spatial distribution of the major ion hydrochemistry in the study area

($r = 0.45$) and a negative correlation of H_2S with Eh values ($r = -0.39$).

Hydrogeochemical facies and water types

Based on the hydrogeochemical data for all analyzed samples, the percentages of major ions were plotted on a Piper diagram (Fig. 3). The dominant cations and anions were identified by using the left and right ternary diagrams, respectively. Concentrations of Ca^{2+}, Mg^{2+}, Na^+, and K^+ are expressed on the left triangle-shaped diagram, while concentrations of HCO_3^-, SO_4^{2-} and Cl^- anions are expressed on the right triangle-shaped diagram. Each water sample has a dominant cation and anion type. The two data points on the two anionic and cationic triangles are combined on the diamond-shaped diagram to indicate specific hydrogeochemical facies and water types.

For cations, water samples were mostly dropped in the zone (b) and zone (c) of the left ternary diagram in Fig. 3, accounting for about 82% of the cation contents, indicating that these mine water samples had the dominance of Ca^{2+} and mixed types. In contrast, a small part of cations was plotted in the zone (d), suggesting that some water samples were identified as Na^+ type. For anions, most of mine water samples were plotted in the zone (f) of the right ternary diagram in Fig. 3, accounting for about 72% of the anion contents, with HCO_3^- as the dominant type, while about 25% of the (c) mixed zone and one sample was of SO_4^{2-} type.

The Piper diagram also showed that alkaline earths ($Ca^{2+} + Mg^{2+}$) and weak acids (HCO_3^-) exceeded the alkalies ($Na^+ + K^+$) and strong acids ($SO_4^{2-} + Cl^-$), respectively, in most mine water samples. In Fig. 3, about 61% of water samples fell in zone 7 of the diamond part, explaining carbonate hardness exceeds 50% of these samples. It implies that the chemical properties of the mine water samples were dominated by Ca^{2+}, Mg^{2+}, and HCO_3^-. Most of the remaining water samples fell in zone 6, which means they were mixed type waters. In this study, mine water samples can be classified into water types with the percentage composition of major ions from 20% meq L^{-1}. The most dominant type was Ca–Mg–HCO_3–SO_4, accounting for 39.3% of the sampling points, followed by Na–Ca–HCO_3–SO_4 (14.3%), Ca–Mg–Na–HCO_3–SO_4 (10.7%) and Na–Ca–Mg–HCO_3–SO_4 (7.1%) water types. The Ca–Mg–HCO_3–SO_4 water type was distributed in the northern, central and western parts (e.g. at Pauline, Joha, NSS sites), while the Na–Ca–HCO_3–SO_4 type dominated in the northern (e.g. Fra site) and northeastern parts (e.g. at Que 1, Que 2, Roter points) and other types of mixed water contributed in the central part of the area (Fig. 2). In addition, about 7% present the Ca–HCO_3 and Ca–Mg–HCO_3 water types of mine water samples. The dominance of these water types may suggest water–rock interaction.

Mechanisms controlling mine water composition

Three major mechanisms controlling water chemistry, including evaporation, rock weathering, and precipitation dominance were evaluated by Gibbs. In 2009, the boundaries of rock weathering dominance were extended by Kumar et al. (2009) further toward higher weight ratios. In recent years, to clearly define the three domains of the water composition controlling mechanisms, many further studies have been carried out (e.g. Ravikumar et al. 2011; Singh et al. 2013; Tiwari

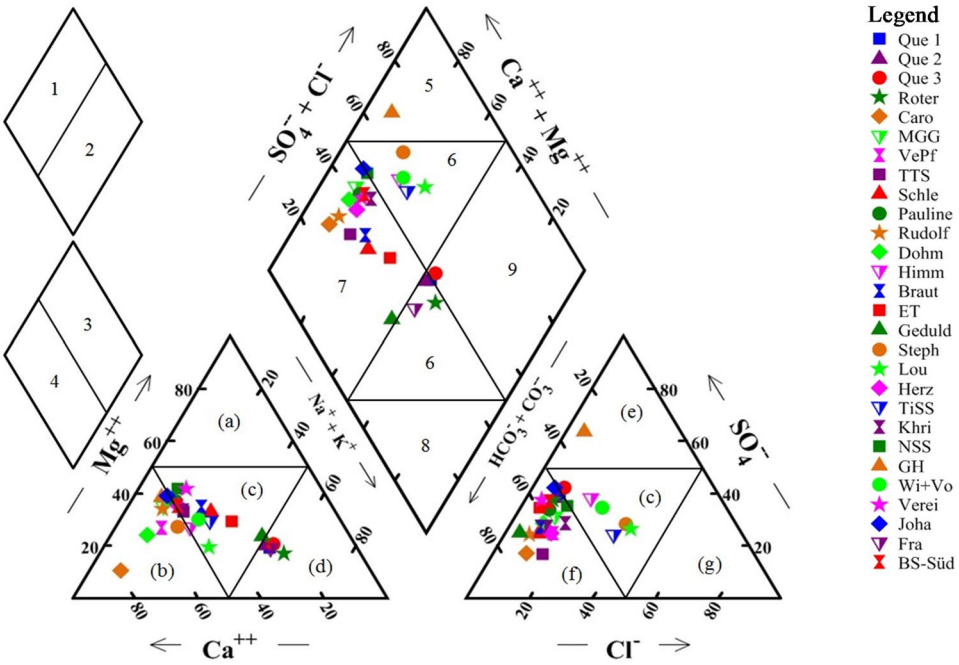

Fig. 3 Piper diagram of mine water samples in the study area: **a** magnesium type; **b** calcium type; **c** no dominant type (mixed zone); **d** sodium and potassium type; **e** sulphate type; **f** bicarbonate type; **g** chloride type. (1) Alkaline earths ($Ca^{2+} + Mg^{2+}$) exceed alkalies ($Na^+ + K^+$); (2) alkalies exceed alkaline earths; (3) strong acids exceed weak acids; (4) weak acids ($CO_3^{2-} + HCO_3^-$) exceed strong acids ($SO_4^{2-} + Cl^-$); (5) non-carbonate hardness exceeds 50%; (6) mixed type; (7) carbonate hardness (secondary alkalinity) exceeds 50%; (8) alkaline earth and weak acids predominated; (9) alkalies and strong acids predominated

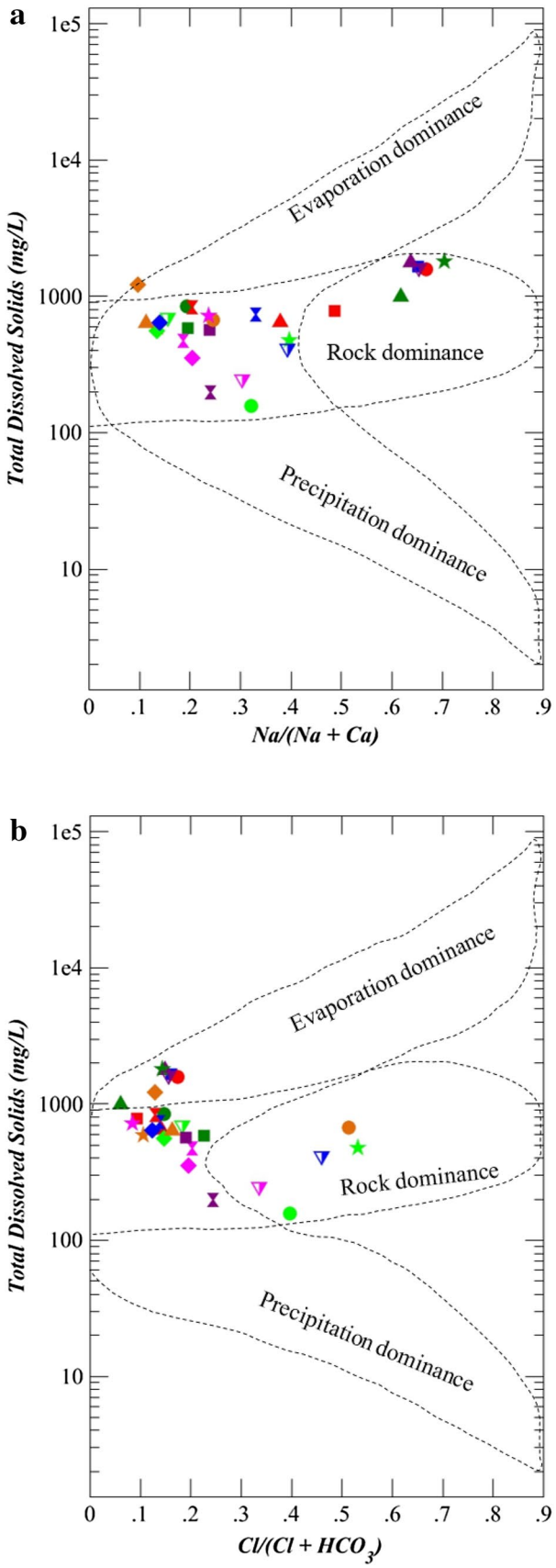

Fig. 4 **a** Gibbs diagram representing the ratio of $Na^+/(Na^+ + K^+)$ (meq L^{-1}) as a function of TDS of mine water samples. **b** Gibbs diagram representing the ratio of $Cl^-/(Cl^- + HCO_3^-)$ (meq L^{-1}) as a function of TDS of mine water samples

et al. 2016a; Wang et al. 2017). The ions depend on some important factors, such as infiltrating rainwater, mineralogical composition and geological structure of abandoned coal mines, dissolution, duration of water–rock interaction, and precipitation of mineral species (Tiwari et al. 2016a).

In the Gibbs cation diagram (Fig. 4a), almost all water samples fell inside the boundary of the rock dominance zone. Values of weight ratio of $Na^+/(Na^+ + Ca^{2+})$ ranged from 0.098 to 0.705 meq L^{-1} (avg. 0.331 meq L^{-1}). This suggested that rock–water interaction was one of the major geochemical processes controlling the dissolved ions of the mine water, while only one water sample dropped outside the boundary of the rock dominance zone.

Similarly, in the Gibbs anion diagram (Fig. 4b), almost all water samples occurred inside the boundary of the rock dominance zone. Values of weight ratio of $Cl^-/(Cl^- + HCO_3^-)$ ranged from 0.062 to 0.533 meq L^{-1} (avg. 0.205 meq L^{-1}). However, a few water samples fell outside the boundary of the rock dominance zone. It indicated the dominant evaporation influence on the mine water chemistry (e.g. Caro, Que 2, Que 3, and Roter samples). Thus, rock–water interaction was a major driving source with the minor influence of evaporation controlling the dissolved ions.

The chemical weathering processes of minerals

Oxidative weathering of sulfide-bearing minerals, such as pyrite (FeS_2) (Favas et al. 2016), as well as dissolution of anhydrite ($CaSO_4$) or gypsum ($CaSO_4 \times 2\ H_2O$) release SO_4^{2-} to mine water (Singh et al. 2010; Tiwari et al. 2016a). In the study area, pyrite, dolomite, calcite and gypsum minerals exist in the sandstones, associated with coal seams (Wisotzky 2017). The overall FeS_2 oxidation reaction produces SO_4^{2-} as:

$$2FeS_{2(s)} + 7O_{2(aq)} + 2H_2O = 2Fe^{2+} + 4SO_4^{2-} + 4H^+. \quad (1)$$

All samples have negative SI_{gyp} values (Table 1). These suggested one possible source of Ca^{2+} and SO_4^{2-} in mine drainage in this area. Simultaneously with the production of SO_4^{2-} ion, the production of acid in coal mine water still continues to occur throughout the pyrite oxidation process (1) in varying quantities (Favas et al. 2016). Hydrochemical results showed the components of mine water with subneutral pH and high sulfate concentrations. Oxidation of released Fe^{2+} may lead to the precipitation of Fe(III) oxyhydroxide ($Fe(OH)_3$) or ochre. This precipitation can form an

orange or yellow sludge coating the bottoms of streams, as at Fra, Que 1, Que 2, Que 3, Roter, Pauline, and Joha points.

HCO_3^- of mine water samples in the study area can be derived from soil zone CO_2. It is produced by the decay of organic matter in the subsurface environment leading to elevated CO_2 pressure (Appelo and Postma 2005). In abandoned coal mines, CO_2 is generated from local organic matter (hard coal, mine timber or carbon dissolved in mine waters) (Thielemann et al. 2004). Thus, mine water with a higher concentration of HCO_3^- (Table 1), can be attributed in environments where more CO_2 may be detected. Moreover, the source of HCO_3^- and Ca^{2+} can be derived from the reaction of silicates by carbonic acid (Appelo and Postma 2005). Results (Table 1) showed that concentrations of HCO_3^- and Ca^{2+} are higher than the concentrations of the other ions. This may partly be explained by the hydrolysis of anorthite which exists in the area (2) (Huang et al. 2018).

$$CaAl_2Si_2O_8 + 2CO_2 + 3H_2O = Al_2Si_2O_5(OH)_4 + Ca^{2+} + 2HCO_3^-. \quad (2)$$

The combination between high concentrations of Ca^{2+}, Mg^{2+}, and HCO_3^- (Table 1), and the wide variation (from 0.325 to 0.809) of the $HCO_3^-/(HCO_3^- + SO_4^{2-})$ ratio in mine water also suggests that coupled reactions involving sulfide oxidation and Ca^{2+}, Mg^{2+}-rich materials dissolution as calcite and dolomite which exist in the rocks of the Upper Carboniferous formations (Wisotzky 2017) control the solute acquisition processes (Singh et al. 2011).

Furthermore, the albite mineral weathering also increases the HCO_3^- concentration in mine water (Lakshmanan and Kannan 2003). Increasing of HCO_3^- concentration compared to the Na^+ concentration (Fig. 5a) implies that HCO_3^- also may be derived from albite mineral weathering (3) as suggested by some scientists (e.g. Fisher and Mullican 1997; Lakshmanan and Kannan 2003).

$$2NaAlSi_3O_{8(s)} + 2H_2CO_3 + 9H_2O = 2Na^+ + 4H_4SiO_{4(aq)} + Al_2Si_2O_5(OH)_{4(s)} + 2HCO_3^-. \quad (3)$$

Otherwise, the plot of $Ca^{2+} + Mg^{2+}$ versus $HCO_3^- + SO_4^{2-}$ (Fig. 5b) of most mine water samples fell along and below the 1:1 equiline, also indicating carbonate weathering (4) and silicate weathering (2) were the dominant processes. However, silicate weathering appears to have occurred more strongly than carbonate weathering (Datta and Tyagi 1996; Lakshmanan and Kannan 2003; Kumar et al. 2009). Thus, these have explained the main source of Ca^{2+} and Mg^{2+} ions to the mine water.

$$CaMg(CO_3)_2 + 2H_2CO_3 = Ca^{2+} + Mg^{2+} + 4HCO_3^-. \quad (4)$$

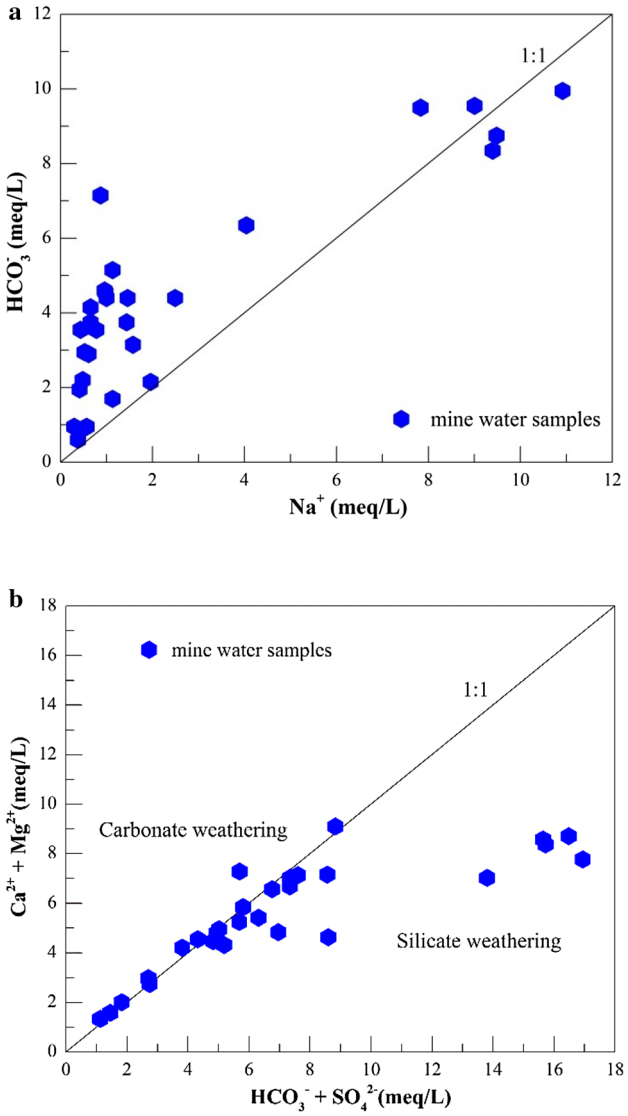

Fig. 5 **a** Na^+ versus HCO_3^- scatter diagram: shows increased HCO_3^- compared to Na^+. **b** $Ca^{2+} + Mg^{2+}$ versus $HCO_3^- + SO_4^{2-}$

Na^+ and K^+ are mainly derived from weathering of aluminosilicate minerals (albite, biotite, muscovite) (Younger et al. 2002). In the study area, the Upper Carboniferous strata contain clay minerals (aluminosilicates). It is concluded that the weathering of aluminosilicate minerals (3), (5), and (6) consumed acidity and released Na^+ and K^+ into the abandoned coal mine drainage.

$$KAl_2(AlSi_3O_{10})(OH)_{2(s)} + H^+ + 3/2H_2O = K^+ + 3/2Al_2Si_2O_5(OH)_{4(s)}, \quad (5)$$

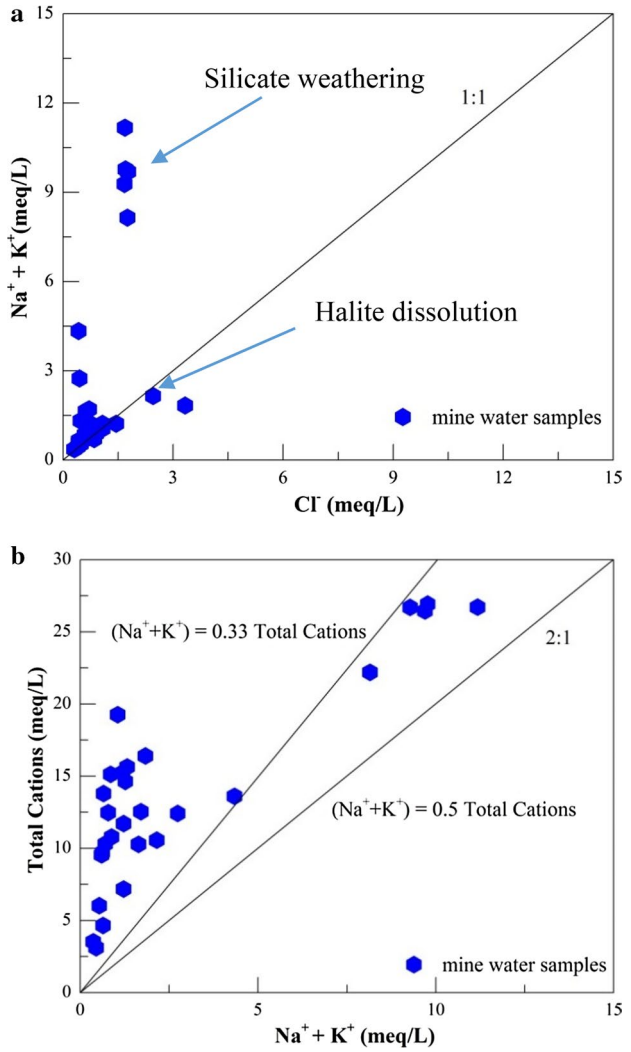

Fig. 6 **a** The plot of $Na^+ + K^+$ versus Cl^-. **b** $Na^+ + K^+$ versus total cations scatter diagram indicates the silicate weathering

$$KMg_{3/2}Fe_{3/2}(AlSi_3)O_{10}(OH)_{2(s)} + 7H^+ + 1/2H_2O = K^+ + 3/2Mg^{2+} + 3/2Fe^{2+} + 2H_4SiO_{4(aq)} + 1/2Al_2Si_2O_5(OH)_{4(s)}. \quad (6)$$

Otherwise, the scatter plot of $Na^+ + K^+$ and Cl^- is shown in Fig. 6a, indicating halite dissolution may be the reaction influencing the mine water chemistry. The $(Na^+ + K^+)/Cl^-$ ratio equals to 1:1 measured in the water samples is attributed to halite dissolution (Fisher and Mullican 1997; Bozau et al. 2017), and can reflect a major source of Na^+ and Cl^- in mine water (Huang et al. 2018). However, a few samples plotted above the 1:1 line, which suggested that halite dissolution was not the decisive process for these samples. Thus, Na/Cl control seems to be exercised by silicate weathering (Fisher and Mullican 1997) and/or ion exchange processes (Bozau et al. 2017).

In addition, the cations contribution to mine water by silicate weathering can also be estimated by the $(Na^+ + K^+)$/total cation concentration ratio (Lakshmanan and Kannan 2003; Glover et al. 2012). According to these scientists, if water samples are dropped above and along the $(Na^+ + K^+) = 0.33$ (TCC) line, suggests that Na^+, K^+ also are derived from silicate weathering (Fig. 6b). However, as explained above, the dissolution of

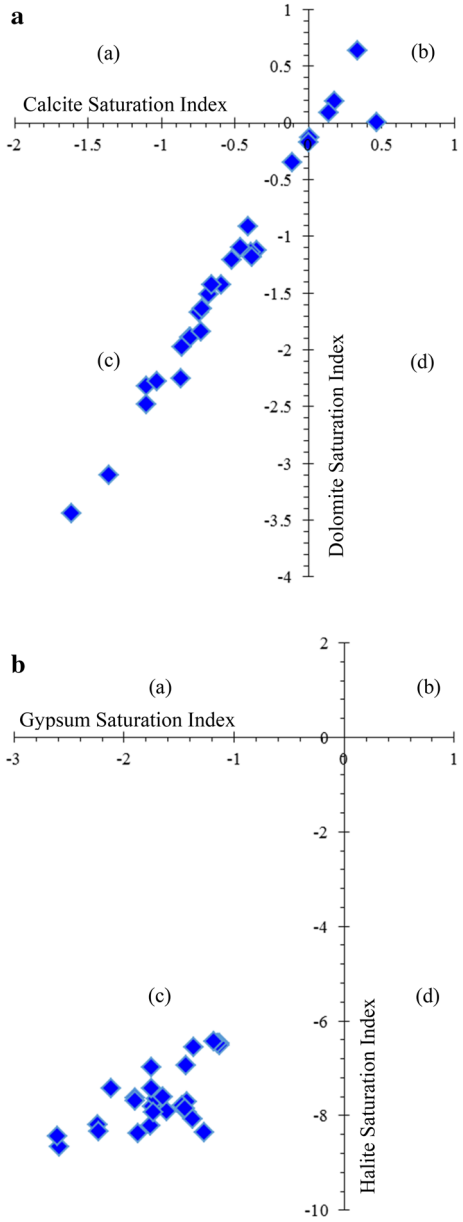

Fig. 7 **a** The relationship between calcite and dolomite saturation indices (a) dolomite saturated and calcite unsaturated; (b) calcite and dolomite saturated; (c) calcite and dolomite unsaturated; (d) dolomite unsaturated and calcite saturated. **b** The relationship between gypsum and halite saturation indices (a) halite saturated and gypsum unsaturated; (b) gypsum and halite saturated; (c) gypsum and halite unsaturated; (d) halite unsaturated and gypsum saturated

halite also may have mainly released Na^+ to mine water and this coincides with $(Na^+ + K^+)/Cl$ ratio in Fig. 6a.

Moreover, Na^+ concentration was relatively elevated in water from the sites Roter, Que 1, Que 2, Que 3 and Fra (Table 1), where feldspars and micas are common minerals in the rocks (GD.NRW-WMS 2017). These sites (with TDS > 1000 mg L^{-1}) can be located along or around the fresh-saline groundwater boundary of regional groundwater in Dortmund and Witten cities, their hydrochemistry might be influenced by deep saline groundwaters rich in Na^+ (Grobe and Machel 2002).

Saturation index (SI) and pCO_2

The saturation state of a water sample can be examined by the following formula (Appelo and Postma 2005):

$$\mathrm{SI} = \log \frac{\mathrm{IAP}}{K_s(T)}, \tag{7}$$

where $K_s(T)$ is the equilibrium constant of reaction considered at the temperature (T), IAP is the ion activity product.

The relationship between the SI_{cal} and the SI_{dol} was plotted in Fig. 7a, between the SI_{gyp} and halite saturation indices in Fig. 7b. The SI_{cal}, SI_{dol} values ranged from − 1.61 to 0.47, and from − 3.44 to 0.64 (avg. − 0.54 and − 1.34), respectively (Table 1). Results indicated that about 82% (SI values < 0) of the water samples were undersaturated with respect to calcite and dolomite (Fig. 7a; Table 1). Calcite and dolomite—if present—will dissolve continuously in these mine waters. Otherwise, only 18% of the samples (SI values > 0) were supersaturated with respect to these minerals, indicating calcite and dolomite will not dissolve further in some samples (e.g. Que 1, Que 2, Roter, and Caro sites), which are located in the northeast of the area.

Moreover, SI of gypsum and halite ranged from − 2.61 to − 1.13, and from − 8.65 to − 6.43 (avg. − 1.68 and − 7.62), respectively. 100% of water samples were undersaturated with respect to gypsum and halite, implying that these minerals may continue to dissolve in mine water (Figs. 7b, 8) if present. However, the SI_{gyp} values were below zero for all samples and tended to move toward zero with increasing TDS value (Fig. 8). This indicated the possibility of gypsum and halite dissolution at water sampling sites.

The pCO_2 values fluctuated between $10^{-2.95}$ and $10^{-1.13}$ atm, with a mean of $10^{-1.63}$ atm. These values were higher than this

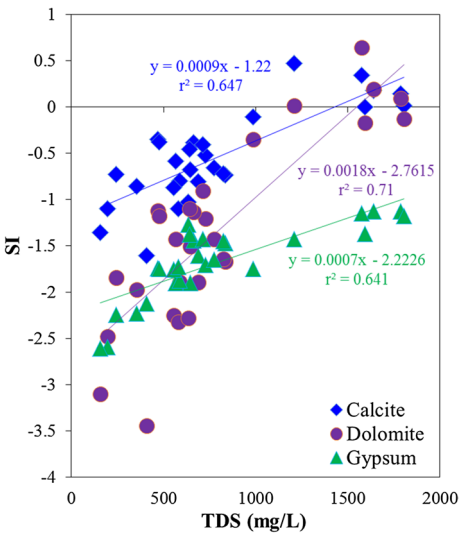

Fig. 8 The plot of TDS versus SI indices values

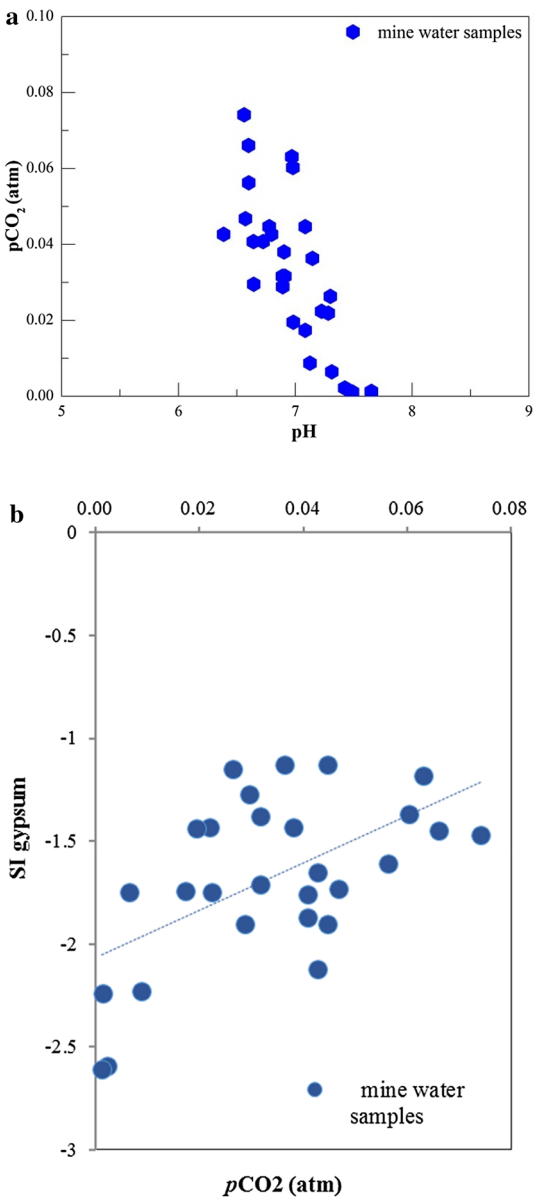

Fig. 9 **a** The scatter plot of pH versus pCO_2. **b** The scatter plot between pCO_2 and SI_{gypsum}

index of the atmosphere (log $pCO_2 = -3.5$ atm) and support potential subsurface silicate and carbonate weathering. CO_2 degassing was expected after discharge from the adits. Figure 9a, b show the decrease of pH with increasing pCO_2, and water samples were progressively more saturated with respect to gypsum when pCO_2 increases, respectively. It indicated that mine waters were not in equilibrium with gypsum during the study period.

Ion exchange process

Two indices of base exchange, namely the chloro-alkaline indices (CAI-1 and CAI-2) proposed by Schoeller (Glover et al. 2012; Li et al. 2013, 2018) were used to explore the possibility of ion exchange (all ions are expressed in meq L^{-1}):

$$\mathrm{CAI}-1=\frac{\mathrm{Cl}^{-}-\left(\mathrm{Na}^{+}+\mathrm{K}^{+}\right)}{\mathrm{Cl}^{-}}, \tag{8}$$

$$\mathrm{CAI}-2=\frac{\mathrm{Cl}^{-}-\left(\mathrm{Na}^{+}+\mathrm{K}^{+}\right)}{\mathrm{HCO}_3^{-}+\mathrm{SO}_4^{2-}+\mathrm{CO}_3^{2-}+\mathrm{NO}_3^{-}}. \tag{9}$$

CAI-1 and CAI-2 (Table 2) positive values suggest that there is a cation exchange between Ca^{2+} and/or Mg^{2+} in the coal mines material with Na^+ and/or K^+ in mine water (10). Otherwise, if values are negative, reverse ion exchange is happening (11) (Glover et al. 2012; Li et al. 2013, 2018) as follows:

$$2\mathrm{Na}^{+}+\mathrm{CaX}_2=\mathrm{Ca}^{2+}+2\mathrm{NaX}, \tag{10}$$

$$\mathrm{Ca}^{2+}+2\mathrm{NaX}=2\mathrm{Na}^{+}+\mathrm{CaX}_2. \tag{11}$$

Most of the calculated CAI-1 and CAI-2 values are negative (account for 75% of samples), except for 7 water samples which have positive CAI-1 and CAI-2 values (25% of samples). This suggested that the ion exchange process releases Na^+ and/or K^+, and Eq. (11) can occur. Moreover, to better understand these processes, the $(Na^+ + K^+)$-Cl^- (meq L^{-1})

Table 2 Calculated CAI-1 and CAI-2 index values for mine water samples

Sample ID	$Ca^{2+}+Mg^{2+}$ (meq L^{-1})	Na^+ (meq L^{-1})	K^+ (meq L^{-1})	$Na^+ + K^+$ (meq L^{-1})	CAI-1	CAI-2
Que 1	8.578	9.482	0.286	9.769	− 4.734	− 0.516
Que 2	8.710	9.004	0.274	9.278	− 4.537	− 0.461
Que 3	8.378	9.395	0.297	9.692	− 4.471	− 0.503
Roter	7.769	10.918	0.253	11.171	− 5.622	− 0.56
Caro	9.103	0.870	0.182	1.052	0.019	0.002
MGG	5.846	0.653	0.133	0.785	0.072	0.010
VePf	4.951	0.779	0.105	0.883	0.021	0.004
TTS	5.248	0.979	0.240	1.219	− 0.137	− 0.026
Schle	4.320	1.435	0.202	1.637	− 1.639	− 0.193
Pauline	7.026	0.957	0.230	1.187	− 0.503	− 0.054
Rudolf	4.472	0.435	0.166	0.601	− 0.421	− 0.037
Dohm	4.547	0.522	0.100	0.622	− 0.224	− 0.025
Himm	2.005	0.566	0.077	0.642	− 0.339	− 0.078
Braut	5.417	1.457	0.248	1.705	− 1.418	− 0.158
ET	4.836	2.492	0.251	2.743	− 5.078	− 0.329
Geduld	4.634	4.041	0.297	4.338	− 9.251	− 0.455
Steph	7.283	1.575	0.258	1.833	0.449	0.257
Lou	4.208	1.957	0.194	2.152	0.123	0.069
Herz	2.744	0.413	0.123	0.536	− 0.118	− 0.02
TiSS	2.981	1.131	0.09	1.22	0.157	0.081
Khri	1.578	0.296	0.069	0.365	− 0.187	− 0.034
NSS	4.799	0.609	0.095	0.704	0.169	0.028
GH	6.570	0.479	0.177	0.655	− 0.517	− 0.033
Wi + Vo	1.333	0.378	0.069	0.447	− 0.133	− 0.037
Verei	7.160	1.131	0.189	1.320	− 1.753	− 0.098
Joha	7.138	0.653	0.205	0.857	− 0.447	− 0.035
Fra	7.026	7.830	0.317	8.147	− 3.643	− 0.463
BS-Süd	6.684	1.000	0.269	1.269	− 0.956	− 0.084

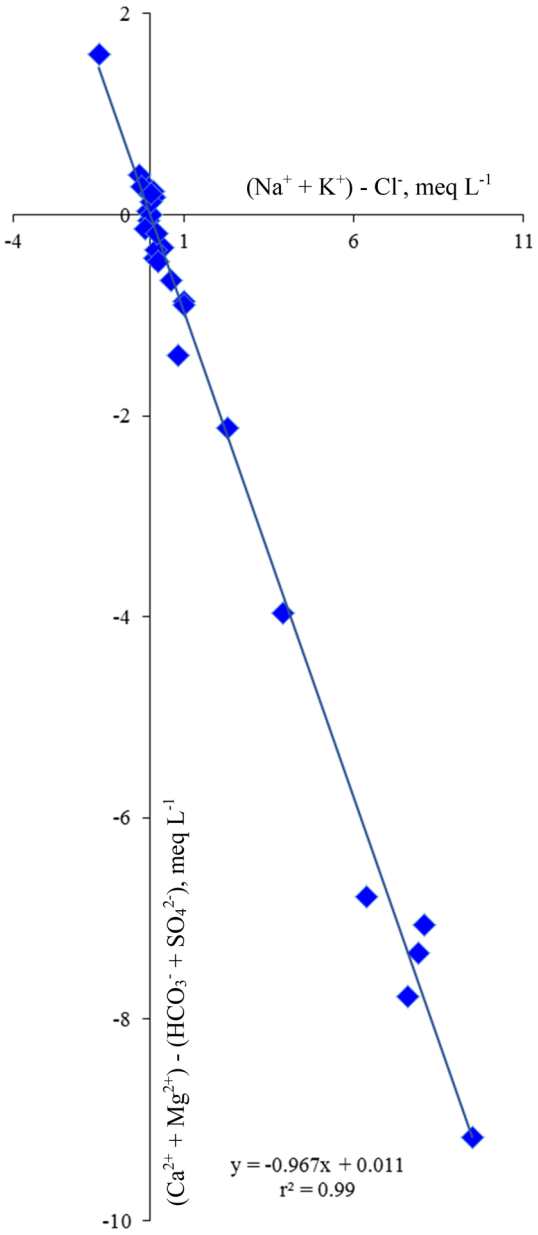

Fig. 10 Scatter plot of $(Na^+ + K^+)$-Cl^- versus $(Ca^{2+} + Mg^{2+})$-$(HCO_3^- + SO_4^{2-})$, meq L^{-1}

and $(Ca^{2+} + Mg^{2+})$-$(HCO_3^- + SO_4^{2-})$ (meq L^{-1}) ratio is estimated by some researchers (e.g. Fisher and Mullican 1997; Glover et al. 2012; Li et al. 2018). If Na^+, K^+, and Ca^{2+}, Mg^{2+} ions are related to each other, the relation of these two parameters should be linear, and a slope of − 1.0. Figure 10 shows that all water samples have a linear correlation ($r^2 = 0.99$), with a slope of − 0.967, implying that these ions participated in the ion exchange reaction. However, the hydrogeochemical data of water samples showed that the total concentration of $Ca^{2+} + Mg^{2+}$ (meq L^{-1}) was higher than $Na^+ + K^+$ (meq L^{-1}) in most water samples. Thus, silicate weathering, calcite, dolomite, and gypsum dissolution processes to release Ca^{2+} and Mg^{2+} ions were the dominant processes in comparison to ion exchange in mine water.

Conclusions

In this paper, hydrogeochemical characteristics of abandoned coal mine drainage in the study area were analyzed through 28 water samples and conclusions are as follows:

Mine water was from weakly acidic to neutral. This study indicated that the TDS and major ion concentrations fluctuated and increased from southern to northeastern parts of the area, relating to water–rock interaction. TDS concentrations showed a significant correlation with EC values. HCO_3^-, SO_4^{2-}, Cl^- and Ca^{2+}, Mg^{2+}, Na^+ ions dominate in the ionic abundances of samples, with the order of the average ion concentrations $HCO_3^- > SO_4^{2-} > Cl^- > NO_3^- > F^-$ and $Ca^{2+} > Mg^{2+} > Na^+ > K^+ > Li^+$; weak acids ($HCO_3^-$) dominate over strong acids ($SO_4^{2-} + Cl^-$), and alkaline earths ($Ca^{2+} + Mg^{2+}$) over the alkalies ($Na^+ + K^+$). Fe^{2+} and H_2S concentrations showed the highest values at Geduld and Fra sites. Ca–Mg–HCO_3–SO_4, Na–Ca–HCO_3–SO_4, Ca–Mg–Na–HCO_3–SO_4, and Na–Ca–Mg–HCO_3–SO_4 water types were the dominant hydrogeochemical facies, with Ca–Mg–HCO_3–SO_4 water type accounting for about 40% of all waters distributed in the northern, central and western parts of the area.

Gibbs diagrams suggested that rock–water interaction was a major factor, with a minor influence of evaporation, controlling the dissolved ions. The SI_{cal}, SI_{dol}, SI_{gyp} and SI halite saturation indices indicated that most samples (82%) were undersaturated, and 18% of the samples were supersaturated with respect to calcite and dolomite. 100% of the samples were undersaturated with respect to gypsum and halite. Silicate weathering, calcite, dolomite, gypsum, and halite dissolution, as well as reverse ion exchange, were the major processes controlling mine water composition.

In the study area, approximately two-thirds of the water sampling sites have yellow or reddish-brown precipitation of iron and some points smell of H_2S. The coal mine water discharge causes visible staining of the receiving streams. These sites are local potentially polluted sources and should be treated accordingly to change hydrogeochemical properties before draining into the receiving streams and the Ruhr river. However, due to the very large amount of water in the Ruhr river, as well as the relatively high pH values and buffer capacity, the pollution of the receiving streams is also locally restricted. This study has been conducted in a short period of time and to enhance the comprehensive understanding of changes in the mine water composition and the environmental impacts of coal mine

drainage in the study area, it is necessary to observe them in the long-term period, also taking parameters, such as trace metals and potential effects of climate change into account.

Acknowledgements The authors would like to thank M.Sc. Sarah Burscheid who helped with sampling in the field. Thanks to Dr. Andrea Hachenberg for advice and discussions, as well as to Mr. Nikolaus Richard and Mr. Oliver Schübbe for laboratory analyses (all in Ruhr University Bochum). We gratefully acknowledge the landlords who allowed access to some adits on their properties. The authors also would like to thank the reviewers for their suggestions and comments that helped to improve the manuscript.

References

Alhamed M (2013) Prognosis of the surface water and groundwater balance of the Lottenbachtal, Bochum, Germany. Ph.D. Dissertation, Ruhr University Bochum

Appelo CAJ, Postma D (2005) Geochemistry, groundwater and pollution. A. A. Balkema Publishers, Leiden

Banks D, Burke SP, Gray CG (1997) Hydrogeochemistry of coal mine drainage and other ferruginous waters in North Derbyshire and South Yorkshire, UK. Q J Eng Geol 30:257–280. https://doi.org/10.1144/GSL.QJEG.1997.030.P3.07

Bigham JM, Nordstrom DK (2000) Iron and aluminum hydroxysulfates from acid sulfate waters. Miner Geochem. https://doi.org/10.2138/rmg.2000.40.7

Bott TL, Jackson JK, Mctammany ME et al (2012) Abandoned coal mine drainage and its remediation: impacts on stream ecosystem structure and function. Ecol Soc Am 22:2144–2163

Bozau E, Licha T, Ließmann W (2017) Hydrogeochemical characteristics of mine water in the Harz mountains, Germany. Chem Erde 77:614–624. https://doi.org/10.1016/j.chemer.2017.10.001

Ceto N, Mahmud S (2000) Abandoned mine site characterization and cleanup handbook. United States Environmental Protection Agency, Washington, DC, p 129

Coldewey BWG, Semrau L (1994) Mine water in the Ruhr area (Federal Republic of Germany). In: 5th international mine water congress, Nottingham (UK), International Mine Water Association (IMWA), IMWA report, pp 613–629

Datta PS, Tyagi SK (1996) Major ion chemistry of groundwater in Delhi area: chemical weathering processes and groundwater flow regime, India. J Geol Soc India 47:179–188. https://doi.org/10.1021/jm030262m

Drobniewski M, Balzer I, Frankenhoff H, Witthaus H (2017) Mine water management in the Ruhr coalfield. In: Mine water and circular economy, IMWA report, pp 183–188

Drobniewski M, Witthaus H (2017) Monitoring of mine water. In: Mine water and circular economy, IMWA report, pp 88–93

Drozdzewski G (1993) The Ruhr coal basin (Germany): structural evolution of an autochthonous foreland basin. Int J Coal Geol 23:231–250. https://doi.org/10.1016/0166-5162(93)90050-K

Drozdzewski G, Schäfer A, Brix MR (2008) Excursion guidebook, 26th regional meeting of the international association of sedimentologists

DWD (2019) Weather and Climate-German Weather Service (Deutscher Wetterdienst). https://www.dwd.de/DE/klimaumwelt/cdc/cdc_node.html. Accessed 2019

Favas PJC, Sarkar SK, Rakshit D et al (2016) Acid mine drainages from abandoned mines: hydrochemistry, environmental impact, resource recovery, and prevention of pollution. In: Environmental materials and waste: resource recovery and pollution prevention. Elsevier Inc., Amsterdam, pp 413–462

Fisher RS, Mullican WF (1997) Hydrochemical evolution of sodium-sulfate and sodium-chloride groundwater beneath the Northern Chihuahuan desert, Trans-Pecos, Texas, USA. Hydrogeol J 5:4–16. https://doi.org/10.1016/j.matchar.2017.04.007

Frankenhoff H, Balzer I, Witthaus H (2017) Mine water concept in detail—a case study of closing a German coal mine at Ruhr district. In: Mine water and circular economy, IMWA report, pp 175–182

GD.NRW-WMS (2017) Geologischer Dienst NRW. https://www.gd.nrw.de/pr_od.htm; and the Web Map Service, 2017. Accessed Dec 2017

Gielisch H (2010) Regional geology of the Ruhr district and remains of the historical mining period in the south of Dortmund and Witten (Carboniferous, Cretaceous, Pleistocene). In: SDGG-GeoTop 2010, international symposium on conservation of geological heritage, 6th, Heft, vol 66, pp 140–144

Glover ET, Akiti TT, Osae S (2012) Major ion chemistry and identification of hydrogeochemical processes of groundwater in the Accra Plains. Elixir Int J Geosci 50:10279–10288

Goerke-Mallet P, Melchers C, Kleineberg K (2016a) Elements and aspects of the post-mining era. Mining report 152 (2016) No. 3

Goerke-Mallet P, Melchers C, Kretschmann J (2016b) Global post-mining challenges—experiences gained from the German hard coal mining industry. In: 16th international congress for mine surveying report, pp 287–292

Gomo M (2018) Conceptual hydrogeochemical characteristics of a calcite and dolomite acid mine drainage neutralized circum-neutral groundwater system. Water Sci 32:355–361. https://doi.org/10.1016/j.wsj.2018.05.004

Grobe M, Machel HG (2002) Saline groundwater in the Münsterland Cretaceous Basin, Germany: clues to its origin and evolution. Mar Pet Geol 19:307–322. https://doi.org/10.1016/S0264-8172(02)00019-3

Harnischmacher S (2010) Quantification of mining subsidence in the Ruhr District (Germany). Hum Impact Landsc Rep 16(3):261–274

Henkel L, Melchers C (2017) Hydrochemical and isotopegeochemical evaluation of density stratification in mine water bodies of the Ruhr coalfield. In: Mine water and circular economy, IMWA report, pp 430–436

Huang X, Wang G, Liang X, Cui L, Mal L, Xu Q (2018) Hydrochemical and stable isotope (δD and $\delta^{18}O$) characteristics of groundwater and hydrogeochemical processes in the Ningtiaota coalfield, northwest China. Mine Water Environ. https://doi.org/10.1007/s10230-017-0477-x

Johnson DB (2003) Chemical and microbiological characteristics of mineral spoils and drainage waters at abandoned coal and metal mines. Water Air Soil Pollut 3:47–66. https://doi.org/10.1023/A:1022107520836

Kgari T, Wyk Y Van, Coetzee H, Dippenaar M (2016) Mine water approach using tracers in South African abandoned coal mines. In: Mining meets water—conflicts and solutions, pp 410–416

Krechetov P, Chernitsova O, Sharapova A, Terskaya E (2019) Technogenic geochemical evolution of chernozems in the sulfur coal mining areas. J Soils Sediments 19:3139–3154. https://doi.org/10.1007/s11368-018-2010-7

Kumar SK, Rammohan V, Sahayam JD, Jeevanandam M (2009) Assessment of groundwater quality and hydrogeochemistry of Manimuktha river basin, Tamil Nadu, India. Environ Monit Assess 159:341–351. https://doi.org/10.1007/s10661-008-0633-7

Lakshmanan E, Kannan R (2003) Major ion chemistry and identification of hydrogeochemical processes of ground water in a part of Kancheepuram district, Tamil Nadu, India. Environ Geol. https://doi.org/10.1306/eg100403011

Li P, Qian H, Wu J, Zhang Y, Zhang H (2013) Major ion chemistry of shallow groundwater in the Dongsheng coalfield, Ordos basin, China. Mine Water Environ 32:195–206. https://doi.org/10.1007/s10230-013-0234-8

Li P, Tian R, Liu R (2018) Solute geochemistry and multivariate analysis of water quality in the Guohua Phosphorite mine, Guizhou province, China. Expo Health. https://doi.org/10.1007/s12403-018-0277-y

Littke R, Ten Haven HL (1989) Palaeoecologic trends and petroleum potential of Upper Carboniferous coal seams of western Germany as revealed by their petrographic and organic geochemical characteristics. Int J Coal Geol 13:529–574

Littke R, Büker C, Lückge A, Sachsenhofer RF, Welte D (1994) A new evaluation of palaeo-heat flows and eroded thicknesses for the Carboniferous Ruhr basin, western Germany. Int J Coal Geol 26:155–183

Lo RS, Gnavi L, Peila D, Suozzi E (2013) Rough evaluation of the water-inflow discharge in abandoned mining tunnels using a simplified water balance model: the case of the Cogne iron mine (Aosta Valley, NW Italy). Environ Earth Sci 70:2753–2765. https://doi.org/10.1007/s12665-013-2335-x

Mayo AL, Petersen EC, Kravits C (2000) Chemical evolution of coal mine drainage in a non-acid producing environment, Wasatch Plateau, Utah, USA. J Hydrol 236:1–16

Müller M (2016) Water drainage in the German coal mining after the close-down in 2018. In: Mining meets water-conflicts and solutions, pp 624–629

Nordstrom DK (2011) Mine waters: acidic to circumneutral. In: Elements report, U.S. Geological Survey, vol 7, pp 393–398

Opitz J, Timms W (2016) Mine water discharge quality—a review of classification frameworks. Proc Int Mine Water Assoc IMWA 2016:17–26

Pope J, Newman N, Craw D et al (2010) Factors that influence coal mine drainage chemistry West Coast, South Island, New Zealand. N Z J Geol Geophys 53:115–128. https://doi.org/10.1080/00288306.2010.498405

Powell JD (1988) Origin and influence of coal mine drainage on streams of the United States. Environ Geol Water Sci 11:141–152

Ravikumar P, Venkatesharaju K, Prakash KL, Somashekar RK (2011) Geochemistry of groundwater and groundwater prospects evaluation, Anekal Taluk, Bangalore urban district, Karnataka, India. Environ Monit Assess 179:93–112. https://doi.org/10.1007/s10661-010-1721-z

Singh AK, Mahato MK, Neogi B, Singh KK (2010) Quality assessment of mine water in the Raniganj coalfield area, India. Mine Water Environ 29:248–262. https://doi.org/10.1007/s10230-010-0108-2

Singh AK, Mahato MK, Neogi B, Mondal GC, Singh TB (2011) Hydrogeochemistry, elemental flux, and quality assessment of mine water in the Pootkee–Balihari mining area, Jharia coalfield, India. Mine Water Environ 30:197–207. https://doi.org/10.1007/s10230-011-0143-7

Singh AK, Raj B, Tiwari AK, Mahato MK (2013) Evaluation of hydrogeochemical processes and groundwater quality in the Jhansi district of Bundelkhand region, India. Environ Earth Sci 70:1225–1247. https://doi.org/10.1007/s12665-012-2209-7

Statistics and IT services NRW (2018) Information and Technology, North Rhine-Westphalia. Census as of 30.6.2018. https://www.it.nrw/statistik/eckdaten/bevoelkerung-am-31122017-und-30062018-nach-gemeinden-93051. Accessed Oct 2018

Stögbauer A, Strauss H, Arndt J et al (2008) Applied geochemistry rivers of North-Rhine Westphalia revisited: tracing changes in river chemistry. Appl Geochem 23:3290–3304. https://doi.org/10.1016/j.apgeochem.2008.06.030

Strehlau K (1990) Facies and genesis of Carboniferous coal seams of northwest Germany. Int J Coal Geol 15:245–292. https://doi.org/10.1016/0166-5162(90)90068-A

Thielemann T, Cramer B, Schippers A (2004) Coalbed methane in the Ruhr Basin, Germany: a renewable energy resource? Org Geochem 35:1537–1549. https://doi.org/10.1016/j.orggeochem.2004.05.004

Tiwari AK, De Maio M, Singh PK, Singh AK (2016a) Hydrogeochemical characterization and groundwater quality assessment in a coal mining area, India. Arab J Geosci. https://doi.org/10.1007/s12517-015-2209-5

Tiwari AK, Singh PK, Mahato MK (2016b) Environmental geochemistry and a quality assessment of mine water of the West Bokaro coalfield, India. Mine Water Environ 35:525–535. https://doi.org/10.1007/s10230-015-0382-0

Tiwari AK, Singh PK, Mahato MK (2016c) Hydrogeochemical investigation and qualitative assessment of surface water resources in West Bokaro coalfield, India. J Geol Soc India 87:85–96. https://doi.org/10.1007/s12594-016-0376-y

Wang L, Dong Y, Xu Z, Qiao X (2017) Hydrochemical and isotopic characteristics of groundwater in the northeastern Tennger desert, northern China. Hydrogeol J. https://doi.org/10.1007/s10040-017-1620-2

Wisotzky F (2017) Water chemistry of the "Erbstollen" waters in the southern Ruhr area. In: Korrespondenz Wasserwirtschaft (KW), p 10 **(in German)**

Wohnlich S (2012) Hydrogeology of the Ruhr Area. Bochumer Geowissenschaftliche Arbeiten, Heft 19(2012):5–13 **(in German)**

Wolkersdorfer CH (2009) Hydrochemistry of mine water discharges in the abandoned Upper Bavarian pitch coal mining district, Germany. In: Water institute of southern africa and international mine water association: proceedings, international mine water conference, pp 823–827. http://www.mwen.info/docs/imwa_2009/IMWA2009_Wolkersdorfer.pdf

Younger PL (1995) Hydrogeochemistry of mine waters flowing from abandoned coal workings in County Durham, England. Q J Eng Geol Hydrogeol 28:S101–S113. https://doi.org/10.1144/GSL.QJEGH.1995.028.S2.02

Younger PL, Banwart SA, Hedin RS (2002) Mine water-hydrology, pollution, remediation. Springer Science + Business Media, Dordrecht

Zieger L, Littke R, Schwarzbauer J (2018) Chemical and structural changes in vitrinites and megaspores from Carboniferous coals during maturation. Int J Coal Geol 185:91–102. https://doi.org/10.1016/j.coal.2017.10.007